

Circumstellar Magnetic Field Diagnostics from Line Polarization

R. Ignace¹ & K. G. Gayley²

¹*Department of Physics, Astronomy, & Geology,
East Tennessee State University, USA*

²*Department of Physics & Astronomy, University of
Iowa, USA*

1 Introduction

Given that dynamically significant magnetic fields in at least some massive stars have now been measured, our contribution addresses the question, to what extent can fields be directly detected in circumstellar gas? The question speaks directly to the very interesting topic of line-driving physics coupled with magnetized plasmas, and how this coupling produces structure in the wind flow. The major goal of this effort is the hope of relating direct measurements of photospheric magnetic fields in massive stars, for example via the methods of Donati & Cameron (1997), with direct measurements of the circumstellar magnetic field from wind lines. Aside from non-thermal emissions, direct detection of magnetic fields derives from the Zeeman effect. Already, Donati et al. (2005) has reported the detection of circularly polarized lines in the disk of FU Ori, signifying that the time is ripe for modeling diagnostics of circumstellar magnetic fields to help guide observers in similar future searches.

We focus our attention on weak-field diagnostics. These come in two main types: the Hanle effect, which pertains to coherence effects for linear polarization from line scattering, and the weak longitudinal Zeeman effect, which pertains to circular polarization in lines.

2 The Hanle Effect for Winds

The Hanle effect refers to how a magnetic field can alter the linear polarization of a scattering line. When the splitting of magnetic sublevels by the Zeeman effect $\Delta\nu_Z$ remains comparable to the natural width of those sublevels $\Delta\nu_N$, a situation of quantum coherence exists. Normally, in the absence of a magnetic field, a coherent scattering line (such as a resonance line) produces linear polarization following a dipole emission pattern (like that of a free electron), but with an amplitude that depends on the details

of the particular transition. In the presence of a relatively weak magnetic field, the magnetic sublevels start to become non-degenerate in energy, leading to an adjustment of the polarization amplitude, which becomes a function of scattering direction with respect to the local magnetic field vector (Stenflo 1994).

A description of this effect in terms of classical damped harmonic oscillators is quite helpful because of its visual nature. For simplicity, consider a level transition that has a polarization amplitude of 100% when scattering through a right angle, just like Thomson scattering. The scattering of unpolarized incident light, typical of the case for illumination by starlight, is pictured as the excitation of two orthogonal dipole oscillators. Forward and backward scattered radiation is unpolarized.

Now consider a magnetic field that is perpendicular to the direction of incident radiation. The magnetic field exerts a Lorentz force on the oscillating bound electron such as to precess the oscillation about the axis of the field direction. The competition here is between the Larmor frequency $\omega_L = g_L B/m_e c$ that sets the rate of precession and the Einstein A -value that sets the rate at which radiation is scattered. For a small ratio of ω_L/A , precession is minimal, and the scattering is essentially non-magnetic. But when ω_L/A is large, precession leads to a full rotation of the oscillator before much damping of the amplitude occurs. Consequently, the scattered light when viewed along the magnetic field becomes completely depolarized. We refer to this limit as “saturated”, because information about the field strength is lost – one knows the field is relatively strong, but the low polarization is a hindrance for determining exactly how strong, yet there is still information about the magnetic field direction. In terms of synthetic polarization spectra from models, the saturated limit is valuable for interpreting the results because of its simplistic properties – complete depolarization along the field, but no precession of the dipole oscillator that is parallel to the field. At its heart the Hanle effect is about redistributing scattered light relative to the zero field case.

There have been a series of papers highlighting applications of the Hanle effect to scattering lines from winds (Ignace et al. 1997; Ignace et al. 1999; Ignace 2001a; Ignace 2001b; Ignace et al. 2004). These have dealt exclusively with line polarizations from optically thin scattering. Ignace et al. (2004) consider the impact of line optical depth on the polarization through a single-scattering approximation, whereby optical depths below unity adopt the single-scattering results, but zero polarization contributions are assumed from regions where the optical depth ex-

ceeds unity. The series has dealt with spherical wind flows, expanding disks, and simplified considerations of oblique magnetic rotators.

A new model presented at this meeting was a calculation for an optically thin line from an axisymmetric Keplerian disk, with results shown in Figure 1. The upper curve shows the total flux emission profile, and the lower curve shows two curves for the polarized line profile. These are plotted against velocity shift normalized to the Keplerian speed at the stellar radius. In the lower panel, the upper curve is the polarization without a magnetic field, and the lower one is with a toroidal field, $B_\varphi \propto r^{-1}$, in the saturated limit. Note that these profiles assume an edge-on viewing perspective and normalized to line optical depth, τ . Going to higher inclinations can affect the profile shape, but the dominant effect is to lower the amplitude of the polarization. Also, this calculation does not take account of absorption of the photospheric continuum, nor contamination by photospheric lines, nor stellar occultation of the rearward disk (e.g., the approach of Ignace 2000). However, with the disk velocity field being right-left anti-symmetric, the effects will be symmetric about line-center.

Of particular interest is that the line-integrated polarization is non-zero, and so even narrow-band polarimetry could be used in order to increase signal-to-noise to detect the influence of the Hanle effect. Different lines that are sensitive to different field strengths would yield not only different levels of polarization, but even net position angle rotations.

There are plans to measure the Hanle effect for the first time in stars other than the Sun. The Far Ultraviolet Spectro-Polarimeter (FUSP, see www.sal.wisc.edu/FUSP; Nordsieck et al. 2003; Nordsieck & Ignace 2005) will have the capability at a resolving power of $R \approx 1800$ of measuring the linear polarization across wind-broadened P Cygni lines of bright stars. This is a rocket payload mission expected to have multiple flights. The stars targeted for detecting the Hanle effect are ζ Ori and ξ Per in the missions second launch, currently scheduled for late 2009.

3 Zeeman Effect for Winds

As is well known, the Zeeman effect describes how a magnetic field leads to splitting of atomic sublevels. In a standard Zeeman triplet, one generally has an unshifted line component that can be linearly polarized (referred to as a “ π ” component) and a pair of equally shifted components left and right of line center range (referred to as “ σ ” components). The

σ components are circularly polarized when viewed along the magnetic field, in which case the unshifted π component will not be seen, but are linearly polarized when viewed orthogonal to the magnetic field.

In the weak-field limit – not so weak as to be in the Hanle regime, but sufficiently weak that the Zeeman splitting is small compared to other broadening processes, the Zeeman components will be strongly blended. In the Hanle regime, the σ components maintain a phase relation, leading to linear polarization effects owing to the coherent superposition of left and right circular polarizations. In the weak Zeeman regime, the σ components are distinctly split relative to their respective natural broadening, and the circular polarizations of the two components add incoherently. Consequently, blending from thermal, turbulent, rotational, or wind broadening strongly diminishes the net circular polarization of the line.

Ignace & Gayley (2003) explored the Zeeman effect in the Sobolev approximation in order to determine the scaling of the circular polarization on magnetic field and wind properties. In the context of the longitudinal Zeeman effect, that relates to the net circular polarization of a line, and scales with the net projected magnetic flux along the line-of-sight, the circular polarization is derived from a Taylor expansion of the difference in intensity between the two σ components. Following that paper, we define I_\pm as left (blueshifted) and right (redshifted) circularly polarized intensities as given by

$$I_\pm \approx \frac{1}{2} I_0(\Delta\lambda \mp \Delta\lambda_B \cos \gamma), \quad (1)$$

where I_0 is the intensity profile shape in the absence of a magnetic field, $\Delta\lambda$ is the wavelength shift from line center, and

$$\cos \gamma = \hat{B} \cdot \hat{z}, \quad (2)$$

for \hat{B} the magnetic field unit vector and \hat{z} a unit vector directed toward the observer. For the intensity of circularly polarized light, we have Stokes $V = I_+ - I_-$, yielding

$$V = -\Delta\lambda_B \cos \gamma \left(\frac{dI_0}{d\lambda} \right)_{\Delta\lambda} \quad (3)$$

In the Sobolev approximation for spherical winds, one builds up a line profile by considering isovelocity surface “cuts” through the wind flow, and integrating the intensities across these surfaces, accounting for stellar occultation and absorption of the photospheric continuum. In the weak-field regime of interest, the fluxes F_\pm are identical in shape but slightly shifted from one another. The difference of these profiles

gives the flux of circular polarization F_V . Focusing on only the emission for illustration, Ignace & Gayley derive the formula:

$$F_V^{\text{emis}}(\Delta\lambda_z) = -\frac{2\pi}{D^2} \int_{\Delta\lambda_z} \Delta\lambda_B \cos\gamma \frac{d}{d\Delta\lambda_z} [S_\lambda (1 - e^{-\tau_S})] p dp, \quad (4)$$

where τ_S is the Sobolev optical depth, $\Delta\lambda_z$ identifies the wavelength shift in the profile from line center that spatially corresponds to an isovelocity zone, S_λ is the position-dependent source function, D is the source distance, and p the polar radius in observer coordinates. Implicit is that the wind is spherical, that the field is axisymmetric, and that the viewer perspective is along the field symmetry axis (otherwise there would be an integration in observer azimuth α since the intersection of the field topology with the isovelocity zones would not generally be azimuthally symmetric). Consequently, equation (4) is maximized for the net magnetic flux through isovelocity zones, and the resultant circular polarizations represent best-case scenarios.

Ignace & Gayley derived polarized line profiles for simplified models of resonance and recombination lines, assuming a velocity law that was linear with radius and using simple field distributions such as a split monopole. As expected, the overall peak amplitude of the polarization scales with v_Z/v_∞ , for v_Z the velocity splitting of the Zeeman components. Peak polarizations of about 0.05% were found, assuming a surface field strength of 100 G and a modest terminal wind speed of 1500 km/s. Such values are challenging, but not beyond the capability of existing and upcoming telescopes, such as the Potsdam Echelle Polarimetric and Spectroscopic Instrument (“PEPSI”, see www.aip.de/pepsi; Hofmann et al. 2002; Andersen et al. 2005).

We are taking steps in developing approaches for computing line polarization for more realistic stellar winds. The two main practical considerations are: (1) what geometries are of most interest and (2) what geometries are most observationally feasible? The answers to both questions would seem to be the same, namely circumstellar disks. Disks in Keplerian (or near Keplerian) rotation are relatively common: for example protostellar disks, interacting binaries, and Be disks. The scaling of polarization amplitude with v_Z/v_{max} , where v_{max} is the maximum flow speed in a system, is robust, and Keplerian disks are limited by the speed of critical rotation of their central star, which is typically a factor of 3 smaller than wind speeds. Consequently, line polarizations will be larger

by a similar factor for a given surface field strength.

As an example, we consider a Keplerian disk with a purely toroidal magnetic field. As noted previously, the isovelocity zones of an axisymmetric rotating disk are left-right symmetric, in contrast to the back-front symmetry for spherically expanding winds. For disks the isovelocity zones are loops. As for the calculation with the Hanle effect, we focus on just the emission contribution and for now ignore absorption and stellar occultation. For modeling the disk emission, we follow the escape probability approach of Rybicki & Hummer (1983).

A useful notational device is to scale the Zeeman splitting to a Doppler shift in the units of an equivalent line-of-sight speed v_Z , and then the simplest preliminary result can be obtained assuming a toroidal disk field obeying $B_\phi \propto r^{-1/2}$. Then the Zeeman shifts of the σ_\pm components, characterized by v_Z , scale in direct proportion to the actual Keplerian speed v_ϕ . As a result, the isovelocity zones for the respective σ_\pm components are identical to Keplerian but with v_ϕ scaled *uniformly* larger or smaller, by $(v_\phi \pm v_Z)/v_\phi$, for each circular polarization.

In this special case, the resultant Stoke-V flux for the line profile is given by the expression

$$F_V^{\text{emis}} = F_+^{\text{emis}} - F_-^{\text{emis}} \quad (5)$$

$$= -2 \left(\frac{v_B}{v_{\text{rot}}} \right) \left[F_I + \Delta\lambda_z \left(\frac{dF_I}{d\lambda} \right) \right], \quad (6)$$

where v_B is v_Z evaluated for a surface field strength at the equator of the star with $B_* = 100$ G, and $v_{\text{rot}} = 500$ km/s is the Keplerian rotation speed at the radius of the star. The resultant profile shape is shown in the lower panel of Figure 2, with the upper panel displaying the Stokes F_I profile for the line emission. The profiles are plotted against observed velocity shift normalized to v_{rot} . Note that the F_I profile shows the characteristic double-peak morphology, whereas the polarized line shows its strongest values at the extreme line wings. The circularly polarized emission from a disk is seen to be left-right *symmetric*, in contrast to a spherical wind that is *antisymmetric* about line center.

4 Observing Strategies

We have emphasized what lies ahead for the future opportunities in direct detection of circumstellar magnetic fields, in order to test models of magnetized plasma flows. It is significant that efforts in this regard are already underway. As mentioned, Donati et al. (2005) have claimed a detection of magnetic

fields in the circumstellar disk of FU Ori. Hubrig et al. (2007) have also claimed a detection of circular polarization in the circumstellar line of a couple of Herbig Ae stars; however, this has been contested by Wade et al. (2006). Eversberg et al. (1999) and St-Louis et al. (2007) have searched for the Zeeman effect in lines of Wolf-Rayet stars, although they have no confirmed detections as yet. The key point is that observers are undertaking these searches, albeit with difficulty. More detections are to be expected, so diagnostic procedures are needed to connect the data with models of magnetized winds and disks.

This raises the obvious question, how are the Zeeman and Hanle effects to be most effectively employed? Bear in mind that the Hanle effect only works for scattering lines, but it is sensitive to quite weak fields, in the range 1–100 G. For hot stars this generally relegates its usefulness to UV spectropolarimetry, which of course requires space-borne instrumentation. Fortunately, FUSP should give us our first opportunity of sampling the Hanle effect in the UV lines of hot stars.

On the other hand, there are limited classes of objects where even $H\alpha$ can act as a scattering line, significant for the fact that it can be observed from the ground, and sensitive to fields of around 1 G. Such sources include yellow hypergiants and some blue supergiants (e.g., Verdugo et al. 2005). Another important class are supernovae, as for example the polarization from $H\alpha$ seen in SN1987A (Jeffery 1987, 1991). Studies of polarization in SNe suggests that observed variations can arise in part from line scattering effects e.g., Hoffman 2006). In those cases where the polarization arises from line scattering, comparisons of the polarizations between different lines and in relation to the continuum polarization from Thomson scattering could reveal the presence of the Hanle effect and thereby constrain magnetic fields in the ejecta of SNe.

The magneto-rotational instability (MRI – Balbus & Hawley 1991) has been found to be a robust mechanism for producing turbulent magnetic fields. In particular in a Keplerian disk, simulations indicate that for an initially vertical field threading the disk, the MRI leads to two primary field components: one that is predominantly toroidal (like that of our model profiles) and one that is turbulent or “randomized”. Moreover, the toroidal field likely switches direction between the upper half disk and the lower half. So for the Zeeman effect, the oppositely directed toroidal field essentially leads to net zero magnetic flux around the disk for optically thin emission, and so would not produce observable circular polarization. This would not be the case for the Hanle effect, as the result

shown in Figure 1 does not depend on the handedness (or reversals) of the toroidal field in the disk.

A distinct advantage of the Hanle effect in *turbulent* magnetic regions is that it is not canceled by line-of-sight magnetic field reversals, the way the longitudinal Zeeman effect is. Indeed, the Hanle effect has been employed as a diagnostic of turbulent solar magnetic fields (Stenflo 1982; Stenflo et al. 1998). (Note however that for an unresolved source, a field that is tangled on a spatial scale that is small compared to the Sobolev length will likely lead to complete depolarization from that region.)

Perhaps the best strategy is to employ the Zeeman and Hanle effects in a complementary fashion. The Hanle effect will likely be best sensitive to weak fields from scattering lines in regions where the line is optically thin (Ignace et al. 2004), even if the surface field is quite strong, because the circumstellar field will typically drop rather rapidly with radius (as for multipole fields). The Zeeman effect will be sensitive to strong photospheric fields, and possibly circumstellar fields in the inner wind or disk. Both of these should be used along with additional sources of information about the source, such as the continuum polarization that may arise from electron scattering, and line profile shapes in Stokes- F_I .

We suggest that one promising target for honing these diagnostics is σ Ori E. This Bp star has a Zeeman detection (Landstreet & Borra 1978), has anomalous X-ray behavior (Groote & Schmitt 2004), and cyclic variations in its $H\alpha$ emission (Townsend et al. 2005), all that been successfully interpreted in terms of a strongly magnetized circumstellar envelope (Townsend & Owocki 2005). This and similar sources where the magnetic field properties are already highly constrained would be good targets for detecting the Zeeman and Hanle effects in circumstellar lines.

The authors would like to thank Ken Nordsieck for discussions of the Hanle effect in SNe, and Jennifer Hoffman for a preview of recent line polarization data in SNe.

References

- Andersen, M., et al. 2005, in High Resolution Infrared Spectroscopy in Astronomy, (eds) Käuff, Siebenmorgen, Moorwood, 57
- Balbus, S., & Hawley, J. 1991, ApJ, 376, 214
- Donati, J.-F., & Collier Cameron, A. 1997, MNRAS, 291, 1

- Donati, J.-F., Paletou, F., Bouvier, J., Ferreira, J. 2005, *Natur*, 438, 466
- Eversberg, T., Moffat, A., Marchenko, S. 1999, *PASP*, 111, 861
- Groote, D., & Schmitt, J. 2004, *A&A*, 418, 235
- Hofmann, A., Strassmeier, K., Woche, M. 2002, *Astr. Nach.*, 323, 510
- Hoffman, J. L. 2006, to appear in *Circumstellar Media and Late Stages of Massive Stellar Evolution*, *RMxAA Conf. Ser.* (astro-ph/0612244)
- Hubrig, S., Yudin, R., Schöller, M., Pogodin, M. 2006, *A&A*, 446, 1089
- Ignace, R. 2000, *A&A*, 363, 1106
- Ignace, R. 2001a, in *Advanced Solar Polarimetry – Theory, Observation, and Instrumentation*, *ASP Conf. Ser.* 236, (ed) Sigwarth, 227
- Ignace, R. 2001b, *ApJ*, 547, 393
- Ignace, R., Cassinelli, J., Nordsieck, K. 1999, *ApJ*, 520, 335
- Ignace, R., Gayley, K. 2003, *MNRAS*, 341, 179
- Ignace, R., Nordsieck, K., Cassinelli, J. 1997, *ApJ*, 486, 550
- Ignace, R., Nordsieck, K., Cassinelli, J. 2004, *ApJ*, 609, 1018
- Jeffery, D. 1987, *Natur*, 329, 419
- Jeffery, D. 1991, *ApJS*, 77, 405
- Landstreet, J., & Borra, E. 1978, *ApJ*, 224, L5
- Nordsieck, K., et al. 2003, in *Polarimetry in Astronomy*, (ed) S. Fineschi, *Proceedings of the SPIE*, 4843, 170
- Nordsieck, K., & Ignace, R. 2005, in *Astronomical Polarimetry: Current Status and Future Directions*, *ASP Conf. Ser.* 343, (eds) Adamson, Aspin, Davis, Fujiyoshi, 284
- Rybicki, G., & Hummer, D. 1983, *ApJ*, 274, 380
- St-Louis, N., 2007, to appear in *Mass Loss from Stars and the Evolution of Stellar Clusters*, (eds) de Koter, Smith, Waters
- Stenflo, J. O. 1982, *Solar Phys.*, 32, 41
- Stenflo, J., *Solar magnetic fields: polarized radiation diagnostics*, 1994, (Dordrecht: Kluwer)
- Stenflo, J., Keller, C., Gandorker, A. 1998, *A&A*, 329, 319
- Townsend, R., Owocki, S. 2005, *MNRAS*, 357, 251
- Townsend, R., Owocki, S., Groote, D. 2005, *ApJ*, 630, L81
- Verdugo, E., et al. 2005, in *The Nature and Evolution of Disks Around Hot Stars*, *ASP Conf. Ser.* 337, (eds) Ignace and Gayley, 324
- Wade, G., et al. 2006, in *Solar Polarization 4*, *ASP Conf. Ser.* 358, (eds) Lites, 369

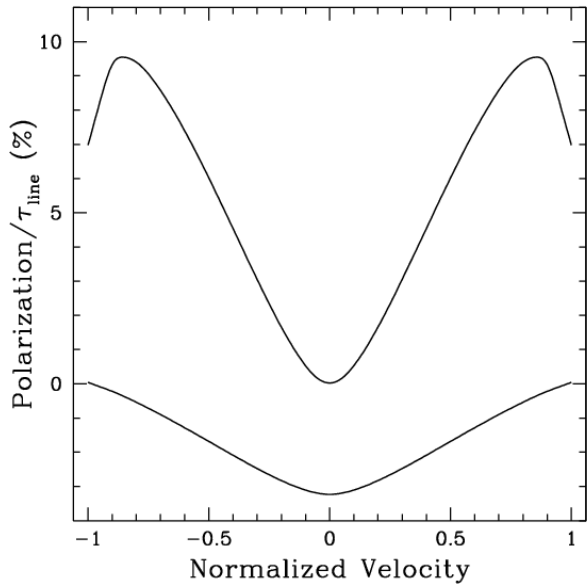


Figure 1: The Hanle effect for a thin scattering line from a Keplerian disk seen edge-on. The polarization is normalized to the line optical depth $\tau_{\text{line}} < 1$. The upper curve shows the polarization without a magnetic field. Lower curve is for a toroidal field in the saturated limit. The sign change signifies a rotation of the polarization position angle by 90° .

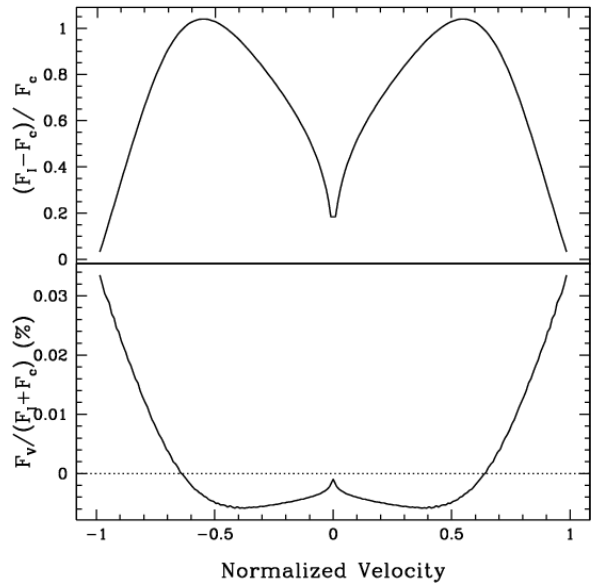


Figure 2: Upper panel shows the emission line profile from a Keplerian disk (relative to and normalized by the continuum level). Lower panel displays the percent circularly polarized profile assuming a toroidal magnetic field with $B_* = 100$ G for an optical line.